

This document was produced  
by scanning the original publication.

Ce document est le produit d'une  
numérisation par balayage  
de la publication originale.

---

Geological Survey of Canada  
Commission géologique du Canada

---

**BULLETIN 372**

**THE ANALYSIS OF THE REMANENCE COERCIVITY  
SPECTRUM BY CONTINUOUS AND ALTERNATING  
FIELDS: RELATIONSHIP BETWEEN COERCIVITY  
AND ALTERNATING FIELDS STABILITY SPECTRA**

Jean L. Roy

1986

**Canada**



**Geological Survey of Canada  
Bulletin 372**

**THE ANALYSIS OF THE REMANENCE COERCIVITY  
SPECTRUM BY CONTINUOUS AND ALTERNATING  
FIELDS: RELATIONSHIP BETWEEN COERCIVITY  
AND ALTERNATING FIELDS STABILITY SPECTRA**

Jean L. Roy

1986

© Minister of Supply and Services Canada 1986

Available in Canada through

authorized bookstore agents  
and other bookstores

or by mail from

Canadian Government Publishing Centre  
Supply and Services Canada  
Ottawa, Ontario, Canada K1A 0S9

and from

Geological Survey of Canada  
601 Booth Street  
Ottawa, Canada K1A 0E8

3303-33rd Street N.W.  
Calgary, Alberta T2L 2A7

100 West Pender Street  
Vancouver, British Columbia V6B 1R8  
(mainly B.C. and Yukon)

A deposit copy of this publication is also available  
for reference in public libraries across Canada

Cat. No. M42-372E                      Canada: \$4.00  
ISBN 0-660-12176-X    Other countries: \$4.80

Price subject to change without notice

## **Preface**

*The alternating field technique has been used in paleomagnetism for over two decades. With the development of magnetic randomizers capable of producing high fields (e.g. the randomizer used at the Geological Survey of Canada) different phases of remanence related to different events, that occurred during the history of a rock unit, can be recognized and often separated.*

*This report describes and compares the results obtained by performing both continuous and alternating field treatments. This experimental work bridges the gap between rock magnetism and paleomagnetism by applying rock magnetic techniques, normally used with artificial samples, to natural rocks. The author also establishes the relationship between the remanence coercivity and the remanence stability to alternating fields.*

*An understanding of the effect of alternating field treatments upon the coercivity spectrum of a natural rock is of fundamental importance in establishing a procedure capable of determining the extent of the spectrum, a requirement that needs to be fulfilled if the alternating field data are to be interpreted correctly. The analysis performed on a wide variety of rock samples indicates that the method could be applicable to any rock type, thus increasing the reliability of the data so widely used for continental drift and tectonic interpretations.*

*R. A. Price  
Director General  
Geological Survey of Canada*

## **Préface**

*La technique des champs alternatifs est employée en paléomagnétisme depuis plus de deux décennies. Avec la mise au point d'appareils de dispersement de vecteurs magnétiques capables de produire des champs élevés (e.g. l'appareil employé à la Commission géologique du Canada), on trouve que différentes phases de rémanence qui se rapportent à différents événements, qui eurent lieu durant la phase d'évolution de la roche, peuvent être reconnues et souvent séparées.*

*Ce rapport décrit et compare les résultats obtenus en effectuant des traitements par champs continus ainsi qu'alternatifs. En appliquant des techniques du magnétisme des roches, normalement employées avec des échantillons artificiels, à des échantillons de roches naturelles, ce travail expérimental ferme l'écart entre le magnétisme des roches et le paléomagnétisme. De très grande importance, en décomposant le segment du rebours de la courbe d'hystérèse, l'auteur établit le rapport dont on avait tellement besoin entre la coercitivité de rémanence et la stabilité de rémanence vis-à-vis les champs alternatifs.*

*Il est essentiel de connaître l'effet des traitements par champs alternatifs sur le spectre des coercitivités d'une roche naturelle afin d'établir une procédure capable de déterminer l'ampleur du spectre, une condition que l'on se doit de rencontrer afin d'interpréter correctement les données de champs alternatifs. L'analyse effectuée sur une grande variété d'échantillons indique que la méthode peut être applicable à n'importe quel type de roche, ce qui augmente d'autant plus la confiance que l'on peut accorder à ces données qui sont utiles à bien des sujets concernant, soit la dérive des continents, soit des interprétations tectoniques au plan local.*

*Le directeur général de la Commission  
géologique du Canada  
R. A. Price*



## CONTENTS

1	Abstract/Résumé
2	Introduction
2	Hysteresis curves
2	The remanence hysteresis curve
2	The back-field curve
4	The remanence coercivity spectrum
5	Interacting fields
7	The $R_{cp}$ curve
8	The remanence a.f. stability
13	Practical applications
13	Additional information
14	Synopsis and conclusion
14	Remanence coercivity
15	Remanence a.f. stability
15	Alternating field treatments
16	NRM detection
16	Terminology
16	Acknowledgment
17	References
00	<b>Figures</b>
3	1a. Remanence hysteresis curves
3	1b. Decay curves of initial remanence
4	2. Remanence vector compositions at different stages of a hysteresis loop
5	3. Complete hysteresis and resulting $R_{rem}$ curves
6	4. $R_{if}$ and $R_{rem}$ curves of siltstone 111C
7	5. $R_{if}$ and $R_{rem}$ curves of gabbro 78A
9	6. Relationship of rc and rafs spectra for siltstone 111C
10	7. Results from siltstone 191B
12	8. Results from greywacke 25C
13	9. Results from siltstone 150B
14	10. Results from gabbro 78A
15	11. Results from different rock types



---

# THE ANALYSIS OF THE REMANENCE COERCIVITY SPECTRUM BY CONTINUOUS AND ALTERNATING FIELDS: RELATIONSHIP BETWEEN COERCIVITY AND ALTERNATING FIELDS STABILITY SPECTRA

---

## Abstract

Comparison of results obtained from a variety of natural rock samples using both continuous and alternating field (c.f. and a.f.) techniques demonstrates the complementary nature and potential of the two techniques. The remanence coercivity spectrum is analyzed by obtaining families of hysteresis curves in c.f. of up to 1200 mT. The extraction of the decay curves from the composite back-field curves reveals several important features: interacting fields among magnetic carriers occur in all rock types investigated including redbeds; the interaction takes place at the low end of the spectrum and its effect is defined by a new parameter — the crossing point; a co-ordinate ( $R_{cp}$ ) of this parameter which varies among, but remains essentially constant within, rock types can be used as a classification index. For most specimens, the remanence (NRM) acquired in the earth's field is only a small fraction ( $10^{-3} - 10^{-4}$ ) of their saturation remanence meaning that the application of the a.f. procedure to recover the NRM must be carefully devised.

Treatments in a.f. up to 290 mT indicate that a.f. is much more effective than c.f. for unlocking remanences. Thus, a clear distinction has to be made between the remanence coercivity (rc) spectrum and the remanence a.f. stability (rafs) spectrum. An effectiveness ratio ( $R_e$ ) of the c.f. and a.f. required to reduce a saturation remanence to a certain level is used to establish a relationship between those two spectra. The  $R_e$  varies with rock types and thus can be used as an identification index; in many instances, the ratio remains nearly constant within the rock type.

The method of combining detailed c.f. and a.f. experiments provides an effective means of ascertaining whether or not the rc spectrum of a natural rock has been investigated in its entirety, — a prerequisite that needs to be met if the a.f. data, so widely used in paleomagnetism, are to be interpreted correctly.

## Résumé

Une comparaison de résultats d'un assortiment d'échantillons de roches naturelles obtenus en employant des techniques de champs continus (c.f.) et alternatifs (a.f.) démontre le caractère complémentaire et le potentiel des deux techniques. Le spectre de la coercitivité de la rémanence est étudié en obtenant des familles de courbes d'hystérèse en champs continus allant jusqu'à 1200 mT. En extrayant la courbe décroissante de la courbe à rebours réellement composée de deux courbes superposées, nous découvrons plusieurs caractéristiques importantes; un phénomène d'interaction de champs parmi les porteurs d'aimantation se produit dans toutes les roches étudiées, même dans les grès rouges; l'interaction a lieu au début du spectre et son effet est défini par un nouveau paramètre: le point de croisement; une coordonnée ( $R_{cp}$ ) de ce paramètre varie d'un type de roche à l'autre mais demeure à peu près constant pour un type en particulier, ce qui implique que  $R_{cp}$  peut être employé comme un indice de classement. Pour la plupart des échantillons, l'aimantation rémanente naturelle (ARN) acquise dans le champ de la terre est une bien petite fraction ( $10^{-3}$  à  $10^{-4}$ ) de l'aimantation de saturation; ce fait nous indique que la procédure à employer dans l'usage du traitement par a.f. pour recouvrir l'ARN doit être conçue avec grand soin.

Des traitements par a.f. allant jusqu'à 290 mT indiquent que le traitement par a.f. est beaucoup plus effectif que le traitement par c.f. pour débloquent les aimantations. Ainsi, une distinction nette et précise doit-être faite entre le spectre de coercitivité de la rémanence (rc) et le spectre de la stabilité de la rémanence au traitement par a.f. (rafs). Un calcul des efficacités respectives du c.f. et du a.f. requis pour réduire une rémanence de saturation à un certain niveau nous permet d'établir un rapport ( $R_e$ ) de grande importance entre ces deux spectres. Le  $R_e$  varie selon le type de roche et peut donc servir comme indice de classification; dans bien des cas, le rapport demeure à peu près constant pour un type de roche en particulier.

La méthode de combiner des expériences détaillées par c.f. et a.f. nous permet de s'assurer si le spectre de coercitivité de la rémanence de la roche naturelle a été examiné dans son entier ou non, c'est une condition préalable nécessaire si l'on espère interpréter correctement les données a.f., tellement employées en paléomagnétisme.



## INTRODUCTION

Alternating magnetic field (a.f.) treatments are commonly used in paleomagnetism. However, the application of the a.f. technique is generally limited in scope, that is, the characteristics of the magnetic constituents of the natural remanent magnetization (NRM) of rock samples are rarely investigated in detail, for a number of reasons as discussed in this report.

On the other hand, much has been learned about the characteristics of a variety of magnetic carriers (e.g. magnetite, titanomagnetite and hematite) from a number of detailed rock magnetic studies (e.g. Dunlop and West, 1969; Dunlop, 1971, 1986; Dankers, 1978, 1981; Levi and Merrill, 1978; Hartstra, 1982a, b; Bailey and Dunlop, 1983) in which saturation remanence is analyzed using both c.f. (continuous or direct field) and a.f. treatments. Although such analyses have been rewarding in rock magnetic studies, they have been neglected in paleomagnetic studies. The reason for the neglect is somewhat obscure. It should be realized, however, that rock magnetic studies are usually performed on powder or synthetic samples made of specific grain-size fractions of known magnetic material while paleomagnetic studies are performed on natural rock samples usually composed of a wide range of grain-sizes of different magnetic materials. Therefore a method of analysis used in rock magnetism may not be as successful when applied to natural rock samples.

Some of the results obtained from a wide variety of natural rock samples using both c.f. and a.f. techniques are presented. Although samples from several rock collections were studied, the examples discussed herein are from samples from two published studies of Siluro-Devonian rock units by Roy et al (1979) and Roy and Anderson (1981). This facilitates correlation with fully described paleomagnetic studies and imparts the potential of the technique. The examples are consistent with results obtained from other collections. A new method of analysis of c.f. results is also introduced.

An attempt is made to elucidate and standardize the terminology used in both rock-magnetism and paleomagnetism. Perhaps because the two fields of research have developed separately to a certain extent, certain terms or parameters may have different connotations. For example, it is not uncommon in a.f. work to have the remanence stability spectrum referred to as the remanence coercive force spectrum. In this report most of the parameters commonly used in both rock magnetism and paleomagnetism are used.

## HYSTERESIS CURVES

According to common usage, hysteresis curves are plots of intensities of magnetization versus the direct, single polarity or continuous fields (c.f.) which produce them. There are three types of hysteresis curves; intrinsic, apparent and remanence. Both the intrinsic and apparent hysteresis curves relate to the magnetization while the c.f. is present. Those two types of curves are not discussed here and readers are referred to, for example, Dankers (1978) for details. In this report, we are

concerned exclusively with the remanence hysteresis curve which expresses the relation between the c.f. applied to a substance and the intensity of the remanence remaining (or locked-in) when the field is reduced to zero.

### *The remanence hysteresis curve*

A remanence hysteresis curve is not a continuous curve but consists of segments (Fig. 1a). The first segment is obtained by subjecting a non- or randomly magnetized sample to a c.f. of  $x$  milliTeslas which is then reduced to zero. The measured intensity is defined here as the acquisition remanence ( $R_{if}$ ), as shown in equation 1 below. The sample is then subjected to a series of incremental steps in fields of opposite polarity, up to  $-x$  milliTeslas. The intensity measured at each incremental step is used to construct the back-field curve (from fourth to third quadrant; Fig. 1a). The return curve (from second to first quadrant; Fig. 1a) is obtained by repeating the procedure with fields in the direction of the initial (positive) polarity.

Normally, in rock magnetic studies, a single set of segments called the saturation remanence hysteresis curve is obtained. The acquisition remanence ( $R_{if}$ ) curve is defined first by measuring the remanence for different values of  $x$  which is increased until all the magnetic carriers of the sample have been saturated. The maximum remanence reached is called the saturation remanence. The other segments — the back-field and return curves — are then obtained following the procedure described above. Parameters commonly used are  $H'_{cr}$  which is the field required to produce half of the saturation remanence on the  $R_{if}$  curve and  $H_{cr}$  which is the field of opposite polarity required to reorient half of the saturation remanence in the opposite polarity, that is, the field at which the observed net remanence on the back-field (and return) curves is equal to zero (Fig. 1a). The definitions of  $H'_{cr}$  and  $H_{cr}$  will be broadened in this report so that those parameters will be applicable to any hysteresis (even non-saturation) curve.

A feature of this investigation is that a family of remanence hysteresis curves (with incremental  $R_{if}$  values) was obtained by completing sets of curves (acquisition, back-field and return) for different values of  $x$  up to a maximum of 1200 mT which is the limit of the electromagnet used. That field was not sufficient to magnetize all magnetic carriers in all instances, particularly in sedimentary samples (Fig. 1). From the trend of the curves, however, the remanence produced in 1200 mT field is estimated to be within 10%, and in most instances within 5%, of saturation remanence.

## THE BACK-FIELD CURVE

It is not generally recognized that back-field curves are composite curves obtained by applying fields which coerce some of the magnetic carriers of the initial remanence  $R_{if}$  to change polarity. This means that any point observed on a back-field curve (Fig. 1a) represents (except at saturation fields) the resultant of two vectors of opposite polarities, one being composed of higher coercivity remanences, the other being

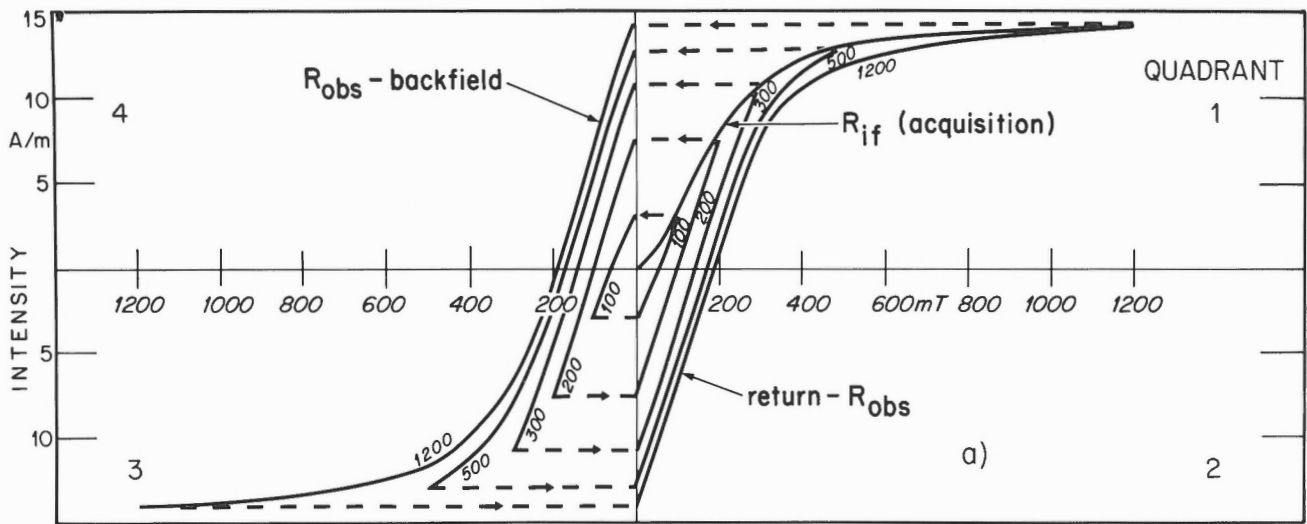


**Figure 1a.** Family of remanence hysteresis curves derived from incrementally higher continuous (direct) fields (c.f.).  $R_{if}$  represents the (initial) remanence acquisition curves produced by the application of a field ( $F_c$ ) of a given magnitude (x mT) to a non- or randomly magnetized sample. Complete hysteresis curves (back-field and return) were obtained for the 100, 200, 300, 500, 700, 900 and 1200 mT incremental steps; the 700 and 900 mT curves are not shown. Remanence observed ( $R_{obs}$ ) on the back-field curves is composite (Eq. 5; Fig. 2). Decomposition of the back-field curves provides one with a means of analyzing in detail the decay of the initial remanence as shown in Figure 1b.

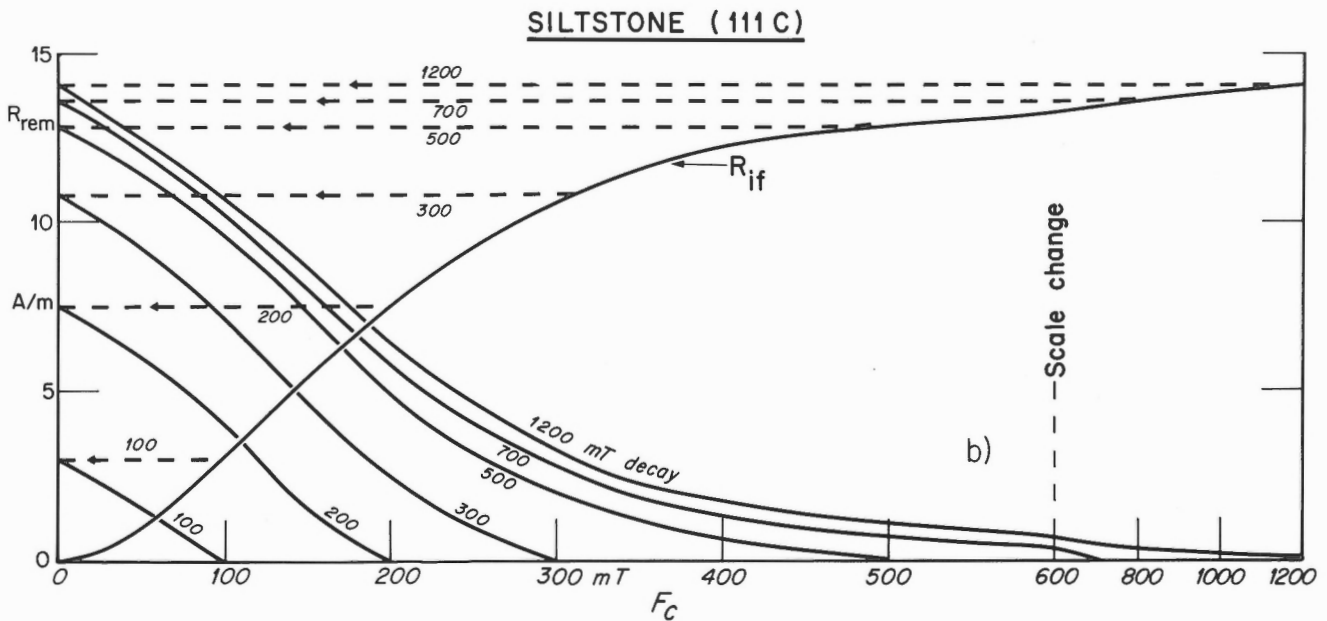


**Figure 1b.** Family of decay curves of the (initial) remanence remaining ( $R_{rem}$ ) upon applying a field ( $F_c$ ) of opposite polarity. These curves are extracted from the curves shown in Figure 1a following Equation 7 and as described in Figure 2. In this report,  $F_c$  is generally referred to irrespective of polarity. As shown in Figure 1a the back-field and return branches are mirror-images so that the relationship between  $R_{rem}$  and  $F_c$  can be obtained equally well from either polarity branch. Thus, in Figure 1b), the  $R_{rem}$  versus  $(-)$   $F_c$  which would normally plot in the fourth quadrant to the left of, or the  $(-)$   $R_{rem}$  versus  $F_c$  which would plot in the (second quadrant), below and inverted with respect to, the  $R_{if}$  versus  $F_c$  (first quadrant) has been reflected upon the latter plot for ease of comparison between the  $R_{if}$  and  $R_{rem}$  curves.

## ANALYSIS OF COERCIVITY SPECTRUM BACK-FIELD METHOD

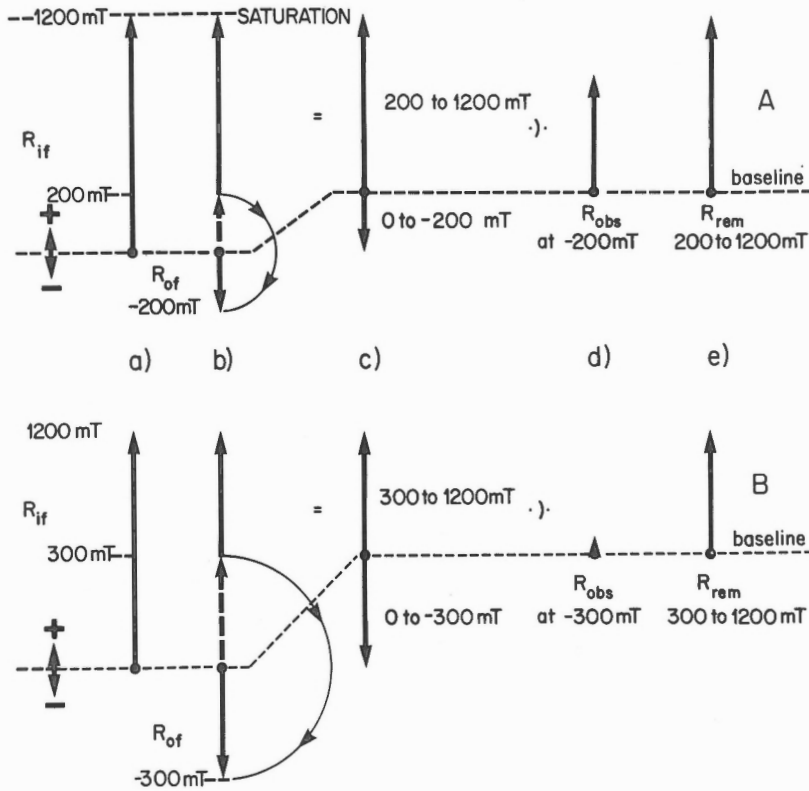


**Figure 2.** Examples of remanence vector compositions at different stages of a hysteresis loop. Upon application of the initial fields, the single polarity (+) remanence  $R_{if}$  is shown at the 200 (A), 300 (B) and 1200 mT (A,B) levels. The subsequent application of 200 and 300 mT in the opposite polarity (-) shown in b) effectively reverses (to  $R_{of}$ ) the vector representing the low end of the coercivity spectrum so that we now have two anti-parallel vectors as shown (in c). The resultant vector observed ( $R_{obs}$ ) is shown in d). The remains of the initial saturation vector (which consists of the higher coercivities) are shown in e). It is interesting to note that  $R_{rem}$  is substantially larger than  $R_{obs}$ . In fact, in B,  $R_{obs}$  is nearly equal to zero although  $R_{rem}$  still contains more than half the saturation  $R_{if}$ .

composed of lower coercivity remanences (Fig. 2). Thus, the back-field curve consists of the superimposition of the decay curve of the initial polarity remanence and the re-acquisition curve of the opposite polarity remanence. Without knowing the respective contribution of the two composing curves, the significance of any features, such as kinks, observed on back-field curves is somewhat uncertain (e.g. Kent and Opyke, 1978; Seguin et al., 1981).

### THE REMANENCE COERCIVITY (RC) SPECTRUM

The analysis of the remanence coercivity (rc) spectrum of a sample thus requires the extraction of the decay curve (Fig. 1b) from the observed back-field curve (Fig. 1a). This is accomplished by writing:

$$R_{if} = \text{intensity of remanence produced when applying the initial c.f. (x}_i\text{mT)} \quad (1)$$

$$R_{of} = \text{intensity of remanence produced by applying a c.f. of opposite polarity} \quad (2)$$

$$R_{obs} = \text{intensity of remanence observed on the back-field curve} \quad (3)$$

$$R_{rem} = \text{intensity of remanence remaining in the direction of the initial c.f.} \quad (4)$$

As illustrated in Figure 2

$$R_{obs} = R_{if} - 2R_{of} \quad (5)$$

$$R_{rem} = R_{if} - R_{of} \quad (6)$$

Combining (5) and (6), we obtain

$$R_{rem} = R_{if} - (R_{if} - R_{obs})/2 = (R_{if} + R_{obs})/2 \quad (7)$$

where  $R_{rem}$  represents that part of the remanence composed of magnetic constituents whose coercivities are high enough to have resisted the coercion exercised by the application of a field of opposite polarity defined here as the coercive field  $F_c$ . As  $F_c$  is made larger, only the magnetic constituents with a higher coercivity level are able to resist the greater coercion and as a result  $R_{rem}$  is smaller. There is, therefore, a relationship between rc and  $R_{rem}$  values and thus decay curves obtained by plotting  $R_{rem}$  against  $F_c$  can be used to analyze the rc spectrum. It is shown here that families of  $R_{rem}$  decay curves derived from incremental  $R_{if}$  values can provide one with much more valuable information than the conventional single curve derived from the saturation remanence.

Certain important features, such as the effect of grain interaction discussed in the following section, are best investigated by normalizing the results for each  $R_{if}$  increment. The normalized curves of siltstone (Fig. 1) and gabbro (Fig. 3) where from equation (7)

$$R_{rem}/R_{if} = (R_{if} + R_{obs})/2R_{if} = 1/2(1 + R_{obs}/R_{if}) \quad (8)$$

are shown in Figures 4 and 5 respectively.

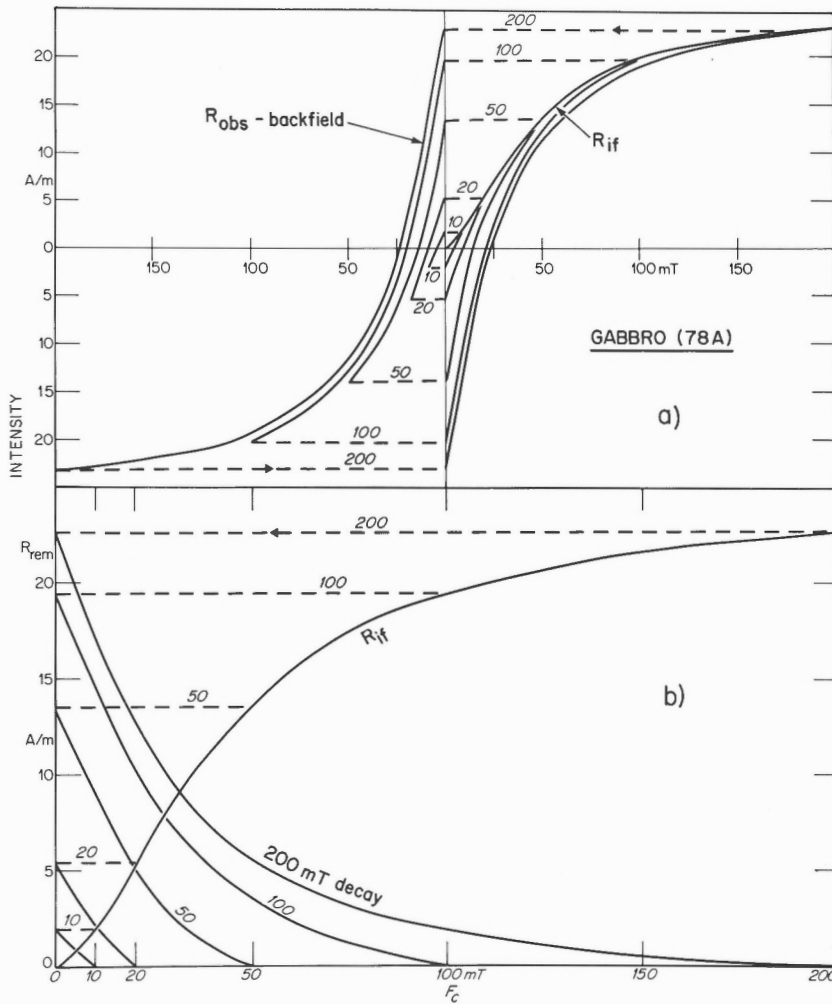


**Figure 3.**

Families of complete hysteresis and the resulting  $R_{rem}$  curves obtained as described in Figure 1. The sample is gabbro 78A from site 4 of Roy et al (1979). Note: for purpose of illustration, the tail ends of the curves have been limited to 200 mT. The coercivity spectrum of this sample extends up to about 300 mT with 1% of the coercivities exceeding 200 mT.

## INTERACTING FIELDS

Several rock magnetic studies performed on artificial samples have shown that the field required to (initially) magnetize a sample from an unmagnetized state is, in general, greater than the field required to magnetize in the opposite polarity the same previously magnetized sample. This was attributed by Dankers (1981) to interaction among magnetic grains producing within the sample a self-demagnetizing field which is opposite to the direction of the initial field (producing  $R_{if}$ ) but parallel to the direction of the opposite polarity field, thereby respectively reducing or enhancing the effectiveness of the applied field.

The effect of grain interaction is usually evaluated from the  $H_{cr}$  and  $H'_{cr}$  of the saturation remanence hysteresis curve. The greater the interacting field, the larger  $H'_{cr}$  must be to compensate for the reduced effectiveness of the applied field

and the smaller  $H_{cr}$  needs to be owing to the enhanced effectiveness of the applied field. Thus, the  $H'_{cr}/H_{cr}$  ratio can be regarded as a qualitative index of interaction among grains (Dankers, 1978).

In this investigation, the definitions of  $H'_{cr}$  and  $H_{cr}$  are broadened by substituting (incremental)  $R_{if}$  (Equation 1) for saturation remanence so that a  $H'_{cr}/H_{cr}$  ratio can be calculated not only for the saturation remanence curve but for any hysteresis curve as shown in Figures 4 and 5. The ratio is readily obtained by taking the field yielding 0.5 (normalized intensity) on the  $R_{if}$  curve over the field yielding 0.5 (normalized intensity) on the  $R_{rem}/R_{if}$  curve which is the field needed to produce  $R_{obs} = 0$  (Equation 8).

The superimposition of curves (Fig. 4, 5) reveals a most useful parameter: the 'crossing point', that is, the point of intersection of the (normalized)  $R_{if}$  and  $R_{rem}/R_{if}$  curves. At

that point, the effect of interaction is compensated for since it is defined by the applied field ( $F_{cp}$ ) which produces the same intensity of remanence ( $R_{cp}$ ) on both the  $R_{if}$  and the  $R_{rem}/R_{if}$  curves. The reducing and enhancing effect of the interactive fields is illustrated by the fact that  $H'_{cr} > F_{cp} > H_{cr}$  as observed in Figures 4 and 5 for all incremental values of  $R_{if}$ . Some estimate of the magnitude of the interacting fields can be obtained by comparing the  $F_{cp}$  co-ordinate (of the crossing point) with  $H'_{cr}$  and  $H_{cr}$ . The  $R_{cp}$  co-ordinate can also be most informative. Without any interaction, the  $R_{if}$  and  $R_{rem}/R_{if}$  curves would be identical with  $H'_{cr} = F_{cp} = H_{cr}$  ( $H'_{cr}/F_{cp} = 1$ ;  $H_{cr}/F_{cp} = 1$ ) and  $R_{cp}$  would occur at 0.5. With interaction,  $H'_{cr}/F_{cp} > 1$  and  $H_{cr}/F_{cp} < 1$  and consequently  $R_{cp}$  occurs below 0.5 (Fig. 4, 5). It can readily be seen from those figures that the higher  $H'_{cr}/F_{cp}$  (and the lower  $H_{cr}/F_{cp}$ ), the lower  $R_{cp}$  is. Therefore,  $R_{cp}$  is a qualitative measure of the effect of interaction, that is, the lower the  $R_{cp}$ ,

the greater the contribution of the interacting fields. One should be aware that in certain specimens, part of the depressed values (below 0.5) could be caused by the possible presence of multidomain grains (Cisowski, 1981).

The results indicate that the interaction is greater (lower  $R_{cp}$ ) for gabbro (Fig. 5) than for siltstone (Fig. 4). The difference in  $R_{cp}$  values is not attributed to the difference in intensities, gabbro having an intensity about twice that of siltstone (Fig. 1, 3). Other siltstone and gabbro samples with different intensities yielded  $R_{cp}$  values similar to those in Figures 1 and 3 (respectively). For example, a gabbro sample from site 10 of Roy et al. (1979) with a saturation intensity of 330 A/m yielded an  $R_{cp} = 0.41$  on the 200 mT curve as compared to the  $R_{cp} = 0.40$  of gabbro 78A (Fig. 5) whose saturation intensity equals 23A/m (Fig. 3). The difference is more likely to be associated with the fact that the coercivity

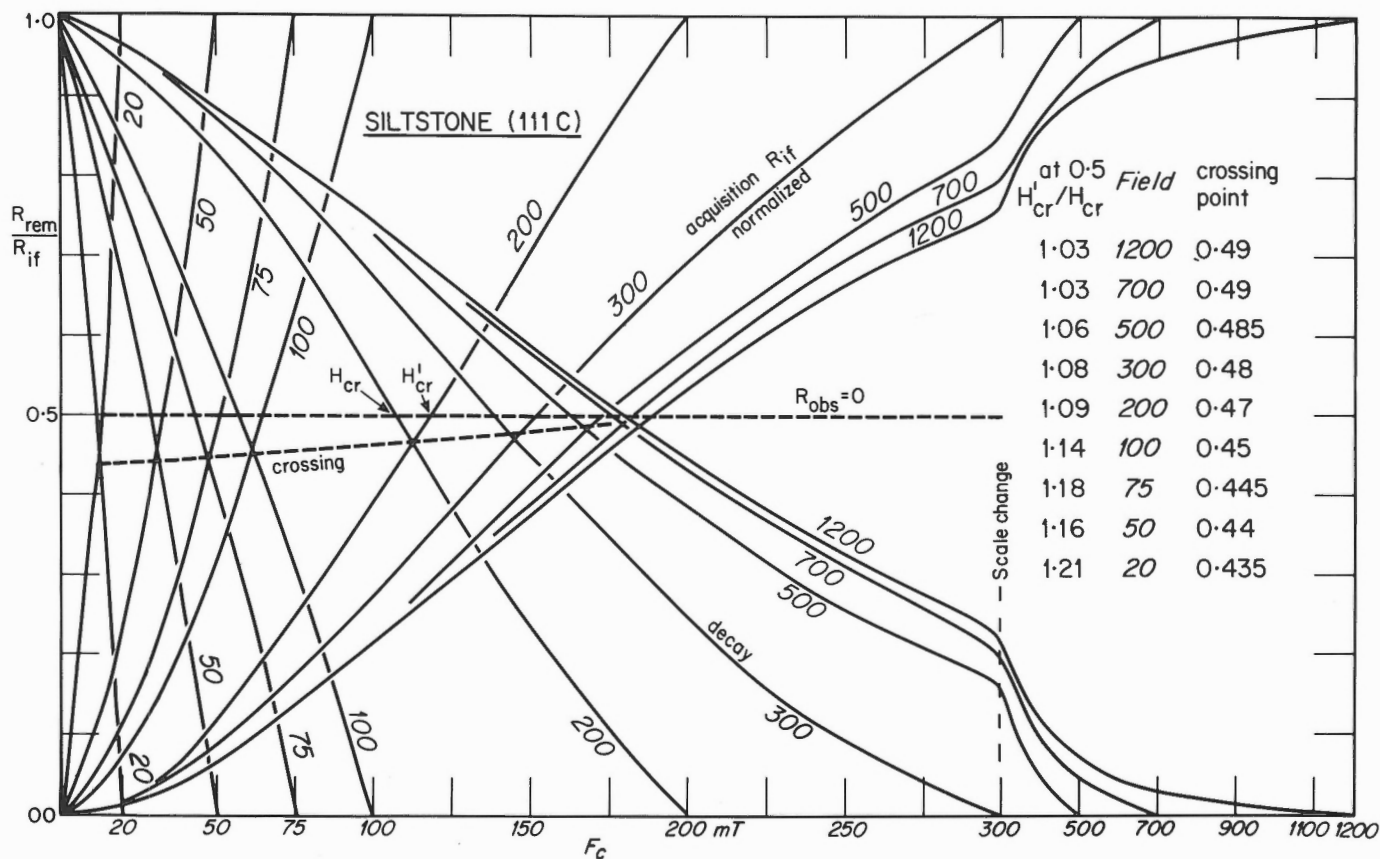


**Figure 4.**  $R_{if}$  and  $R_{rem}$  curves of siltstone 111C (Fig. 1) normalized for each increment of  $R_{if}$  (Equation 8). This type of diagram readily exhibits features that are of great importance for the study of the rc spectrum. The  $H'_{cr}/H_{cr}$  ratio can be obtained for any hysteresis curve by taking the respective fields at which the acquisition curve and its corresponding decay curve cross 0.5 (normalized intensity). The values for each of 9 incremental  $R_{if}$  values are tabled. Most importantly, this diagram puts in evidence a new parameter — the 'crossing point' curve — which yields informative data about the interactive fields within the sample which apparently are present even in a predominantly hematite bearing sample such as this siltstone. The results of this study as a whole indicate that interaction takes place mainly at the low coercivity end of the spectrum.

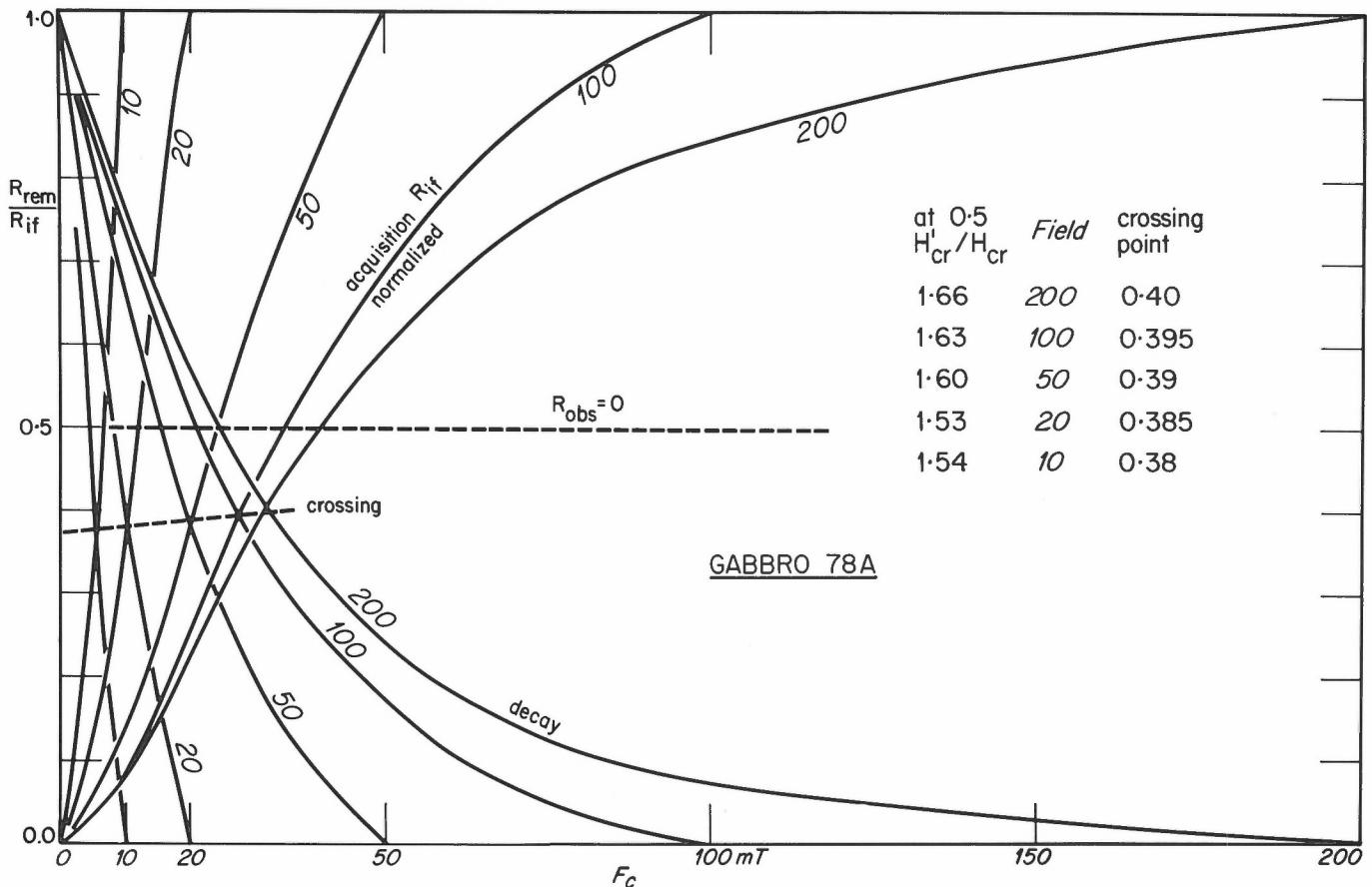


**Figure 5.**  $R_{if}$  and  $R_{rem}$  curves of gabbro 78A (Fig. 3) normalized for each increment of  $R_{if}$  (Equation 8). It is suggested that the  $R_{cp}$  co-ordinate of the crossing point could be used as a classification index. Compare the tabled crossing points with those in Figure 4.

spectrum is more constrained for gabbro than for siltstone, e.g., 99% of the coercivities are below 200 mT for gabbro (Fig. 3) while only 50% of them are below the same level for siltstone (Fig. 1). This clustering of intensity vectors with coercivities towards the low end of the spectrum effectively enhances the effect of interaction. Further data and analyses are required to establish a more quantitative relationship of the interactive fields among different rock types with the possibility of using a "crossing point" index to determine their magnetic properties.

### THE $R_{CP}$ CURVE

The crossing point method reveals a relationship between the inferred interactive fields and the rc spectrum. For both siltstone (Fig. 4) and gabbro (Fig. 5) the effect of the interactive fields is greater (lower  $R_{cp}$ ) for lower coercivities: the siltstone exhibiting a well defined  $R_{cp}$  curve of 0.435 to 0.49 and the gabbro a curve of 0.38 to 0.40. These nearly linear curves tending towards a value of 0.5 are found in all samples studied.

Before discussing the significance of these trends, it is noted that these results are consistent with results obtained

from artificial samples (Dankers, 1978). Using samples of homogeneously distributed hematite grains, Dankers found that the  $H'_{cr}/H_{cr}$  ratio derived from saturation remanence hysteresis curves (produced in fields reaching 2000 mT) was near unity. The  $H'_{cr}/H_{cr}$  ratio of the siltstone with most of the remanence being carried by hematite (Roy and Anderson, 1981) nears unity as the field is increased; at 1200 mT, it is 1.03 (Fig. 4). The  $H'_{cr}/H_{cr}$  ratio of 1.54 to 1.66 measured for gabbro (Fig. 5) for which some of the remanence is carried by magnetite (Roy et al, 1979) falls within the range of 1.3 to 1.7 for artificial samples of dispersed magnetite obtained by Dankers (1978), Hartstra (1982b), and Dunlop (1986). These agreements are auspicious for the useful correlation of results from artificial and natural samples. For the moment, comparisons must be confined to results derived from (near) saturation remanence hysteresis curves because those types of curves are presently the only data available from artificial samples.

The use of incremental values of  $R_{if}$  provides one with an effective means to analyze the rc spectrum in some detail by isolating its low end. The trend towards 0.5 of the  $R_{cp}$  curves (Fig. 4, 5) indicates that the ability to react to interacting fields is predominant among carriers with low coercivities, and diminishes as the carrier coercivity increases.

Thus, it is concluded that for natural rocks whether they are composed of mostly hematite carriers (siltstone) or magnetite carriers (gabbro), the effect of interacting fields resides principally in the low coercivity carriers. If this is correct and because of the relationship between the cancelling factors of continuous and alternating fields (as shown later), then there are serious implications regarding the treatment procedure in low alternating fields as shown below.

## THE REMANENCE A.F. STABILITY (RAFS)

Alternating field (a.f.) treatments have been used in paleomagnetic studies for over two decades. Historically, they were used to cancel a soft (low a.f. stability) component of remanence to recover a hard (high a.f. stability) component of remanence. Typically, in a number of studies, it was found that a component of remanence whose direction was commonly subparallel to the direction of the present field (at the sampling locality) could be cancelled by treatment in a.f. of 10 to 20 mT. Such 'soft' components were (and still are) commonly attributed to recent overprinting (Lapointe et al., 1978). The remanence remaining after treatment in a.f. of 20 to about 60 mT (commonly the highest field then available in many laboratories) was deemed to have been acquired at the time of formation of the rock and regarded as 'primary' remanence (Black, 1964).

With the development of a.f. apparatus capable of producing higher fields (up to 300 mT) has come the realization that the interpretation of a.f. data may not be as simple as that enunciated above (Buchan et al, 1977; Roy and Lapointe, 1978). For example, it has been found that rocks commonly carry more than one remanence of high stability meaning that the remanence remaining after a.f. treatments of 20 to 60 mT may be composed of two or more remanences (e.g., Buchan and Dunlop, 1976; Roy and Robertson, 1978). It is axiomatic that to interpret a.f. data correctly, the magnetic record contained in the rock must be investigated in its entirety meaning that all constituent remanences have to be, at least, recognized and, if possible, separated. Unfortunately, this is not always accomplished and it is probable that some of the remanences, especially those of high stability, often remain unnoticed or unreported for a variety of reasons: a.f. treatments insufficiently high to uncover high stability remanences, uncertainty about the reliability of high a.f. results owing to technical difficulties or inadequate procedure, lack of knowledge and misconception about the effect of alternating fields on remanence coercivity, and confusion caused by a terminology which is misleading. All these problems are interrelated and examined below.

It is commonly stated that a rock sample has been gradually 'demagnetized' by a.f. 'demagnetization'. This can be erroneously construed as meaning that the remanence has been gradually removed. In fact, a.f. treatments do not remove any remanence; on the contrary, they can easily produce some as shown later. When a rock sample is subjected to an a.f. treatment, the magnetic vectors of carriers with coercivities below a certain level tend to follow the direction of the field, that is, they become unlocked and flip-flop between the dual

direction of the alternating field. Upon smoothly reducing the alternating field to zero in the absence of a continuous field, the magnetic vectors will lock into new directions as their carrier coercivity levels are successively met. Ideally, the treatment will produce a randomization of vector directions resulting in an apparent cancellation (resultant vector = 0) of the remanences held by the carriers with coercivities below that certain level. By subjecting the rock sample to treatments in successively higher alternating fields ( $F_a$ ), the randomization is gradually raised to higher coercivity levels. The remanence vector measured after a treatment step represents that part of the remanence composed of magnetic constituents whose coercivities are high enough to resist unlocking when subjected to the applied  $F_a$ . It is important to note that, for any  $F_a$ , the remanence measured is only a fraction of the total remanence, the other fraction consisting of a vectorially cancelled (?) remanence. Thus, the successful separation of remanences of different coercivities is highly dependent upon achieving repeatedly (i.e. after each treatment step) a high degree of randomization of the magnetic constituents with the lower coercivities, a goal, which as shown later, becomes increasingly difficult to reach as the ratio of low/high coercivities increases.

There is much confusion in the literature about the meaning of 'coercivity' and 'stability' as applicable to remanence. Even though a.f. treatments can be used to separate remanences of different coercivities, they do not provide one with a measure of coercivities per se. Rock magnetic studies have shown that, for many magnetic carriers, results obtained from a.f. and c.f. experiments are clearly different meaning that an a.f. decay curve, for example, cannot be assumed *a priori* to be representative of the remanence coercivity spectrum. Therefore, in this report, a clear distinction is made between remanence coercivity (rc) defined by c.f. data (as discussed in previous sections) and remanence a.f. stability (rafs) defined by a.f. data (as discussed in this section).

The only parameter commonly used to quantify a.f. results is the field required to randomize (or vectorially cancel) half of the initial remanence. This parameter is usually referred to as the median destructive field. Commonly used symbols to describe this value are  $H_{1/2I}$  when the initial remanence is the saturation remanence (rock-magnetism) and MDF when the initial remanence is the NRM (paleomagnetism). Realizing that 'destructive' is a misnomer (see above), this parameter is renamed as MRF (median randomizing (or vectorially cancelling) field). To distinguish between saturation and NRM, one can write  $MRF_S$  and  $MRF_N$  respectively.

The significance of  $MRF_S$  is very restricted. This parameter merely indicates the field required to randomize half of the rafs spectrum of a single (polarity) remanence. It does not provide one with any detailed information about the rafs spectrum and its relationship with the rc spectrum. As for  $MRF_N$  values, they are usually meaningless and can often be misleading because NRM values are commonly composed of more than one remanence. Hence, in Figure 6 the  $MRF_N$  (0.005 A/m) is found at a field as low as 65 mT although a substantial portion ( $\approx 20\%$ ) of the remanence has a stability

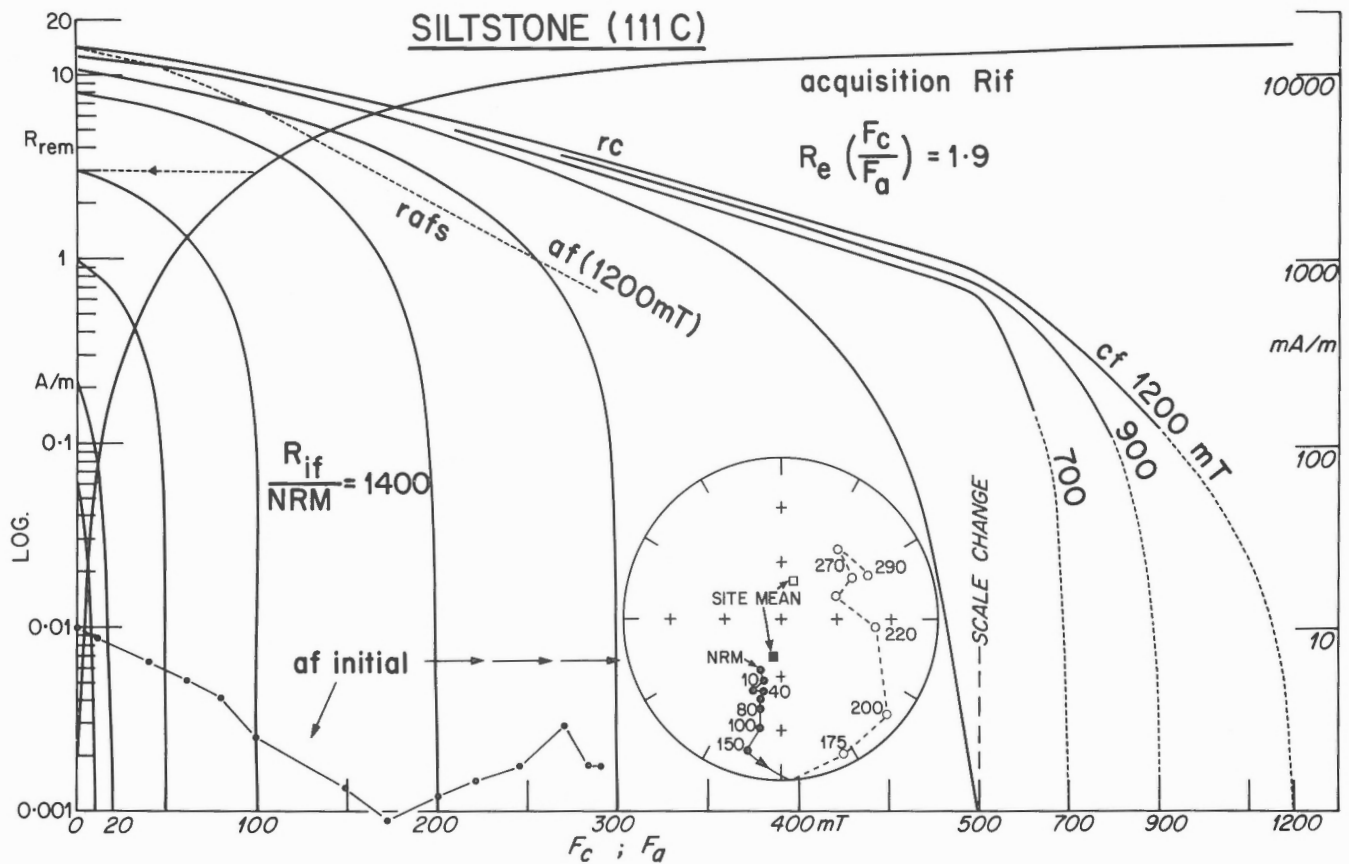


**Figure 6.** Two important correlations are revealed in this type of diagram. First, the  $R_{if}$  and  $R_{rem}$  curves obtained from the c.f. experiments (Fig. 1) are reproduced on a semi-logarithmic scale for comparison with the (non-normalized) results obtained from the initial treatment of the NRM by alternating fields (a.f.). The same abscissa scale is used for plotting the results obtained by applying a continuous field ( $F_c$ ) or an alternating field ( $F_a$ ). Comparison of the  $R_{if}$  curve with that of 'a.f. initial' shows strikingly that during the a.f. treatment the sample is subjected to fields potentially able to produce remanences several hundred to several thousand times larger than the naturally imprinted (and sought) remanences. This means that the a.f. procedure must be carefully devised to randomize as much as possible the remanences produced during the treatment. The  $R_{if}/NRM$  ratio shown in this and other figures is a measure of the relative intensities of saturation  $R_{if}$  over the observed NRM prior to treatment. The ratio measured here indicates that this specimen was originally magnetized in the earth's field to only 0.07% of its saturation value. During a.f. treatment, the ratio of potential/sought remanences does, of course, vary. The ratio can be obtained by measuring the intensities of the  $R_{if}$  and the a.f. initial values at the respective  $F_c$  and  $F_a$  taking into account the effectiveness ratio  $R_e$  discussed below. For example, the intensity on the a.f. initial curve at  $F_a = 200$  mT is 0.0012 A/m and the intensity on the  $R_{if}$  curve at  $F_c = (R_e \times 200 \text{ mT}) = 380$  mT is 12 A/m for a potential/sought ratio = 10 000 meaning that the randomizing factor must substantially exceed 10 000 if the remanence with a rafs of 200 mT is to be accurately defined. Vector direction changes obtained during a.f. initial are shown in the stereonet. Closed (open) symbols indicate positive (negative) inclinations. The squares indicate the mean direction obtained from 12 specimens of site 18 from which this specimen originates.

Second, after the c.f. experiments (Fig. 1), the saturation remanence was reproduced by subjecting the sample to a  $F_c$  of 1200 mT. The sample was then subjected to incremental  $F_a$  up to 290 mT. The smooth decay curve obtained is shown and identified as a.f. (1200 mT). The vector directions (not shown) remained within  $2^\circ$  of the direction of the  $F_c$  applied along the axis of the specimen (for further explanation on vector direction behaviour, see Fig. 8b). An effectiveness ratio ( $R_e$ ) can be determined by calculating the respective  $F_c$  and  $F_a$  required to reduce the remanence to a certain level. For this sample, the  $R_e$  is virtually constant (1.9) throughout the full range investigated (up to  $F_a = 290$  mT).  $R_e$  establishes a clear relationship between remanence coercivity (rc) and remanence a.f. stability (rafs).



exceeding 290 mT (even though the resultant intensity vector at 175 mT dips to less than 10%). In Figure 7, the  $MRF_N$  (0.003 A/m) is apparently reached as low as 15 mT. Further treatment, however, reveals that the 0.003 A/m value is reached again at 115 mT on the ascending leg of an apparent increase in intensity (owing to the presence of opposite polarity remanences). Clearly,  $MRF_N$  values can be useless for describing the rafs spectrum of the remanences contained in these specimens. Therefore,  $MRF_N$  should not be used unless it has been established that the rafs spectrum has been investigated in its entirety and the decay curve experiences a continuous and smooth decrease.

Usually, the extent of a rafs spectrum is not easily established. This is commonly attributable to uncertainties regarding the reliability of the data points as the treatment field is increased. Irregular vector changes (and non-smooth intensity decay curves) are often observed as the treatment exceeds 50-100 mT (see examples given). These could be attributable to a number of causes: overlapping rafs spectra of either two distinct remanences or a dual polarity remanence, a small ratio of NRM/remaining remanence, a weak remaining remanence resulting in a small signal/noise ratio for the measuring instrument, improper procedure during a.f. treatment, etc. Alternatively, it is possible that the upper limit of the rafs

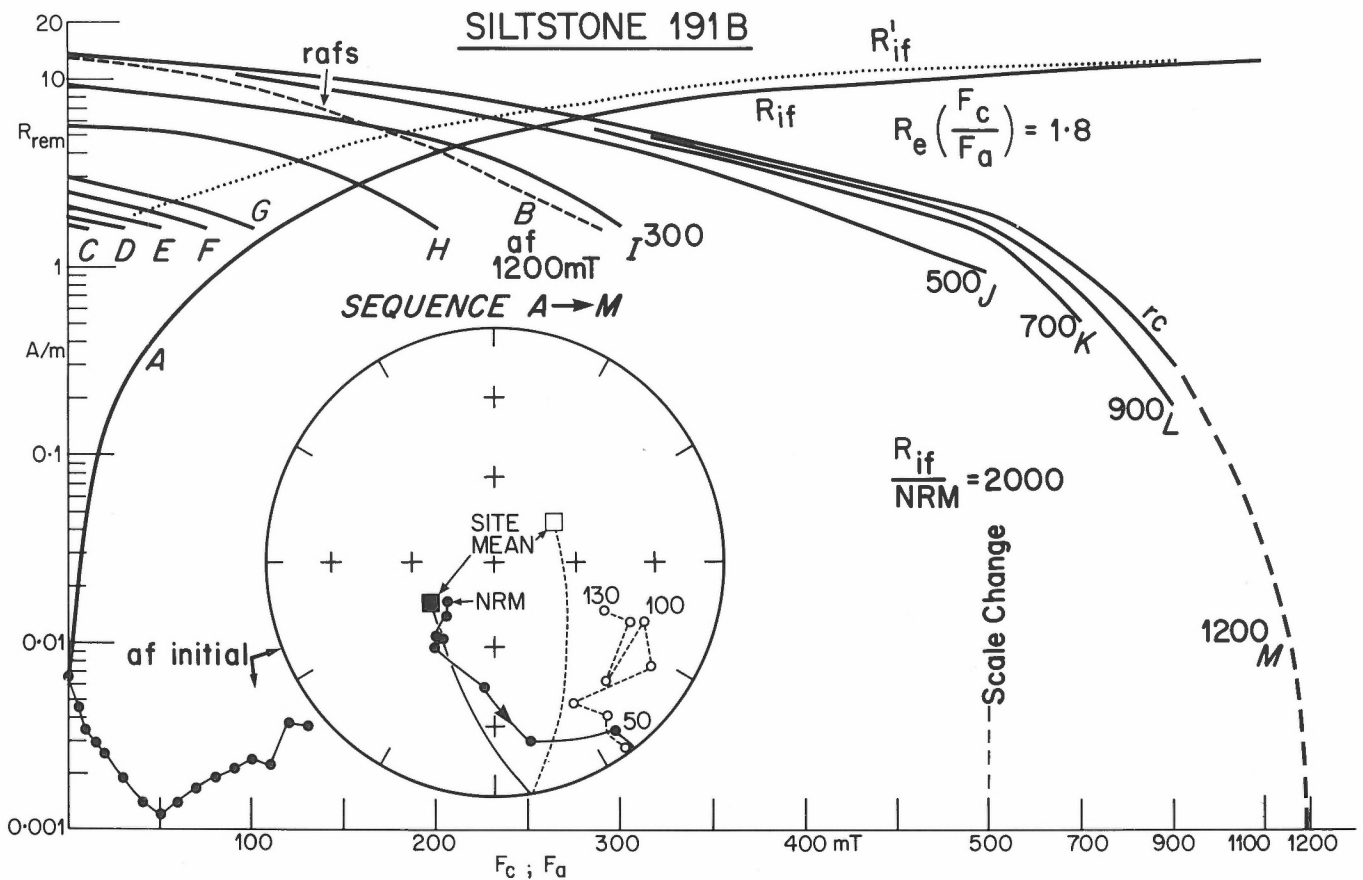


**Figure 7.** Results obtained from a.f. initial treatment (both intensity decay curve and vector direction changes), incremental  $F_c$ , and incremental  $F_a$ . However, one important change distinguishes this Figure from Figure 6: the sequence of experiments was changed as indicated. The a.f. decay curve (B) was obtained immediately following the initial acquisition ( $R_{if}$  curve; A). This was then followed by the series of c.f. experiments which produced the second acquisition (incremental  $R'_{if}$  — with the baseline at 1.55 A/m) and related back-field curves from which the  $R_{rem}$  curves were derived. Comparison of results with those of Figure 6 indicates that the relationship ( $R_e$ ) holds independently of the sequence used in performing the c.f. and a.f. experiments. The sample is from site 29 of Roy and Anderson (1981) and the site mean is based on 15 observations.

spectrum was reached in previous treatments and that the last data points are the result of spurious remanences produced during or after treatment. Consequently, it is difficult to ascertain, from the a.f. results alone, if the rafs spectrum has been uncovered in its entirety and, if so, where the upper limit is.

One method to assess the possible extent of a rafs spectrum is to verify a prerequisite, that is, the rock must contain some magnetic carriers with coercivities sufficiently high that their remanence remains unaffected (stable) up to a corresponding a.f. treatment. This means that a relationship must be established between rc and rafs.

The  $R_{rem}$  decay curves provide one with an excellent means for comparing the rc and rafs spectra of any unidirectional remanence. The results obtained for siltstone (Fig. 1) are reproduced in Figure 6 on a logarithmic scale (for reasons given in the Fig. 6 caption). Following the experiments in c.f. which provided us with the  $R_{if}$  and  $R_{rem}$  curves, the specimen was remagnetized in the c.f. of 1200 mT to reproduce the same saturation remanence with a direction parallel to the axis of the specimen. Then it was subjected to a.f. treatments up to 290 mT using an a.f. randomizer with a 3-axis tumbler (Roy et al., 1973). Throughout all (18) treatment steps, the direction remained within  $2^\circ$  of its initial direction (inclination  $90^\circ$ ) and the intensity decayed regularly with all data points being within 5% of the best fit curve shown in Figure 6.

The a.f. curve lies below the c.f. curve indicating that a.f. treatments are more effective than c.f. treatments in cancelling out (at least part of) the  $R_{if}$  produced by a c.f. of 1200 mT. Indeed, to reduce  $R_{rem}$  to any level (within the range investigated; up to a  $F_a$  of 290 mT), the alternating field  $F_a$  required is always less than the  $F_c$  needed. By measuring the respective  $F_a$  and  $F_c$  required to reduce the  $R_{rem}$  to a certain level, one can define an effectiveness ratio  $R_e (F_c/F_a)$  and thereby establish a relationship between rc and rafs. For example, in Figure 6, a horizontal line drawn from  $R_{rem} = 1$  A/m crosses the 1200 mT decay curve at 490 mT ( $F_c$ ) and the a.f. decay curve at 260 mT ( $F_a$ ) giving an effectiveness ratio of 1.9. For this specimen, the  $R_e$  value is constant throughout the 290 mT rafs spectrum within 5% for all values of  $R_{rem}$ .

The relationship between the rc and rafs spectra was further investigated by changing the sequence of experiments. For siltstone 111C (Fig. 6), the a.f. decay curve was obtained after the c.f. experiments. For siltstone 191B from site 29 (Roy and Anderson, 1981), the  $R_{if}$  curve for fields up to 1200 mT was obtained first to be followed by the delineation of an a.f. decay curve (Fig. 7), with the direction remaining within  $3^\circ$  of the applied field. This was then followed by the series of c.f. experiments with incremental fields (10, 20... 1200 mT). The result was a superimposed incremental  $R'_{if}$  and accompanying set of hysteresis curves from which  $R_{rem}$  decay curves were derived (Fig. 7). None of the decay curves reached zero except for the 1200 mT curve. This is owing to the fact that the specimen was previously subjected to a field  $F_c$  of 1200 mT (first  $R_{if}$ ) which then imposed a remanence of 13 A/m. The results indicate that the  $F_a = 290$  mT treatment has randomized 88% of the remanence. The remaining (12%)

unidirectional remanence (1.55 A/m) is evidently composed of carriers with very high coercivities; the 10 to 30 mT (C to I) curves all terminate at the 1.55 A/m level indicating that these carriers have coercivities higher than 300 mT, at least, and probably in excess of 400 mT as can be estimated from the prolongation of a baseline at the 1.55 A/m level.

The change in procedure does not appear to have substantially altered the relationship between the rc and rafs spectra when both are derived from the same saturation remanence. The effectiveness ratios for both specimens 111C and 191B remain constant; the small difference in  $R_e$  (1.9 and 1.8; Fig. 6, 7) is not attributed to the change in procedure. Specimens from that collection indiscriminately yielded  $R_e$  values of 1.8 and 1.9 indicating that the sequence in which the a.f. and c.f. experiments are performed is apparently unimportant.

The results (Figure 6, 7) illustrate one of the technical difficulties associated with a.f. treatment of the NRM and the paramount importance of the procedure employed. It is evident from the a.f. initial results that, as the field is increased, irregular vector changes are observed, especially in Figure 7. The occurrence of such irregularities is not surprising when one considers the  $R_{if}/NRM$  ratios or compares the (rapidly rising)  $R_{if}$  curve with the a.f. initial curve. For example, when specimen 191B (Fig. 7) is treated in a  $F_a = 100$  mT, all carriers with coercivities lower than  $R_e \times 100$  mT are unlocked. This means that a remanence with a potential intensity of 3.5 A/m ( $R_{if}$  at  $F_c = 180$  mT) has to be randomized to obtain an accurate determination of the sought remanence; such a potential remanence is 1400 times larger than the remanence of 0.0025 A/m observed at  $F_a = 100$  mT (for  $F_a = 50$  mT, the ratio potential/observed remanence is 1000). Therefore, the randomizing factor of the a.f. apparatus has to be extremely high and great care must be given to the procedure to be used. This is illustrated by describing the different procedures used for siltstones 191B (Fig. 7) and 111C (Fig. 6).

Procedure A used for siltstone 191B was a linear decay rate with time periods of 40 s for the 5 to 50 mT (10mT/80 to 8 s) treatments and incremental time period increases to, for example, 2 min for 130 mT (10 mT/9 s). For siltstone 111C, the decay time rate was similar in high fields (e.g., 4 minutes for 290 mT = 10 mT/8 s) but upon reaching 100 mT, the decay time rate was reset to lengthen the decay from 100 to 0 mT to 4 minutes thereby reducing the decay rate from 10 mT/8 s to 10 mT/24 s in order to improve the randomization of the magnetic vectors with low coercivities (procedure B). Comparison of results obtained from the two procedures clearly shows that, in general, vector changes are much less irregular when using procedure B (e.g., compare stereograms in Figures 6 and 7). Thus, it is concluded that those irregularities observed after treatment in high a.f. really originate from the low coercivity remanences. In hindsight, this is to be expected since as found in this investigation (e.g., Fig. 6-9) the ratio  $R_{if}/$ remaining initial (or sought) remanence is commonly in the order of 1000 to 10 000. For this reason, a linear decay rate with a time period proportional to the maximum field (10 mT/8 s; procedure A) is apparently inadequate in

many instances. It is suggested that a decay rate approaching a logarithmic decrease is much preferable. It is worth noting that the a.f. frequency may play an important role in the required decay time. The frequency used for the experiments described here was 60 Hz. A higher frequency such as 400 Hz used in some apparatuses should improve the randomization.

It is important to note that the rafs spectrum and the associated  $R_e$  are both dependent upon the effectiveness of the a.f. apparatus utilized. Comparing results obtained with this randomizer in the tumbling and non-tumbling mode,

Park (1984) has shown that the efficacy ratio of tumbling over non-tumbling is 1.2. Thus, had the randomizer been employed in a non-tumbling mode rather than the tumbling mode, the rafs spectrum would lie between the rc spectrum and the rafs spectrum delineated here. Evidently, the  $R_e$  would have been smaller, being proportional to the tumbling/non-tumbling ratio, as, for example, with the silstone samples with  $R_e$  values of 1.5 to 1.6 instead of 1.8 to 1.9 in Figures 6 and 7. Likewise, gabbro samples with predominant magnetite remanences yield  $R_e$  values of 2.3 to 2.5 in a

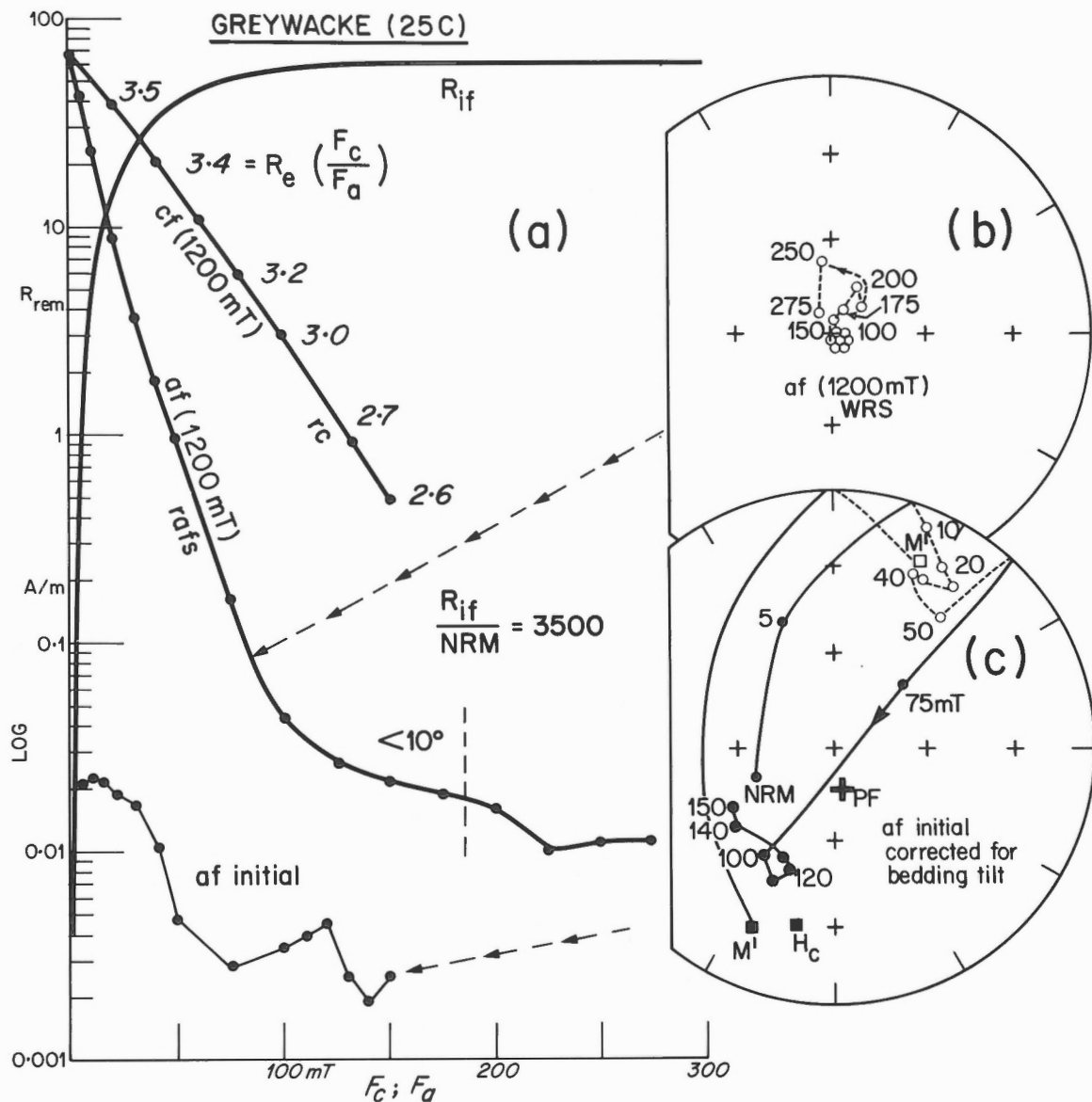


**Figure 8.** Results from a greywacke from site 15 of Roy and Anderson (1981). The a.f. initial treatment indicates that the NRM is composed of (at least) three remanences as shown in (c); the site mean direction (squares) of two of the remanences —  $M'$  and  $H_c$  — are shown. The direction of the remanence with the highest rafs ( $>50$  mT) is difficult to determine accurately rendering its existence perhaps questionable. However, the a.f. (1200 mT) curve clearly shows that the sample contains carriers with rafs as high as 275 mT. The vector directions obtained during a.f. treatment are shown in (b). The  $F_c = 1200$  mT was applied along the axis of the specimen and would plot at the centre of the stereonet. Up to  $F_a = 175$  mT, the vector remains within  $10^\circ$  of the initial direction (as indicated by the vertical dashed line on the rafs curve) but large deviations occur in higher fields, up to  $25^\circ$  at 250 mT.



$T_{UB}$ , that both magnetite and hematite carriers were present at that site (Roy et al., 1979). The increase in  $R_e$  is attributable to the rapid decay rate of the a.f. curve relative to the c.f. curve in the interval  $F_a$  of 50 to 140 mT. The noticeable kink occurring at 140 mT probably represents the (gradual) transition from the dominant magnetite rafs spectrum (<140 mT) to the dominant hematite rafs spectrum (mostly >140 mT). Of interest is the fact, that in the results obtained so far, a specific ratio appears to be associated with a certain rock type. For example, gabbro samples have  $R_e$  values of 2.3 to 2.5 (Fig. 10, 11) and siltstone samples have  $R_e$  values of 1.8 to 1.9 (Fig. 6, 7, 9, 11). Generalization should be avoided at this early stage but it would be most useful if  $R_e$  values could be used as a rock type index.

## SYNOPSIS AND CONCLUSION

The results indicate that a clear distinction needs to be made between remanence coercivity and remanence response to

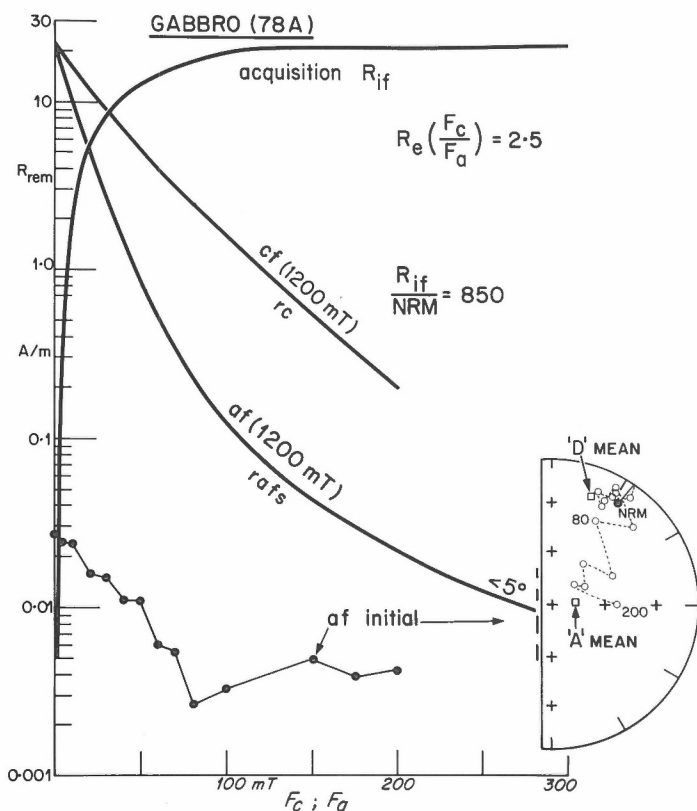


**Figure 10.** Comparison of the results of the gabbro (Fig. 1) with those of the NRM. The a.f. initial results show that the sample was carrying two remanences: A and D. Remanence A has a rafs exceeding 80 mT. The a.f. (1200 mT) curve shows that only 1% of the saturation remanence has a rafs spectrum exceeding 80 mT. Comparison of the  $R_{if}$  and a.f. initial curves shows that the potential/sought ratio exceeds 4500 (for  $F_a > 80$  mT). This demonstrates that the a.f. technique can be used to uncover relatively small remanences. During the a.f. (1200 mT) experiments, the direction remained within  $5^\circ$  of the initial direction. The mean A and D directions obtained for this rock unit are shown.

alternating fields. Thus an attempt has been made to adapt the terminology to reflect the reality. Continuous field results are used to define the remanence coercivity while a.f. results are used to establish the stability of remanence when exposed to a.f. treatments, that is, to establish the remanence a.f. stability. While making full use of some of the terms commonly employed (e.g.  $H'_{cr}$ ,  $H_{cr}$ ), others specifically chosen to enhance the distinction between c.f. treatments (e.g.  $F_c$ ,  $F_{cp}$ ,  $R_{cp}$ ,  $R_{if}$ ) and a.f. treatments (e.g.  $F_a$ , MRF) are being proposed.

One of the main features of this study is the dual role of the  $R_{rem}$  curves — i.e. the (c.f.)  $R_{rem}$  and the (a.f.)  $R_{rem}$  — which permit us to establish the much needed relationship between coercivity and stability by correlating the rc and rafs spectra.

The principal conclusion drawn from this study are summarized below.

### Remanence coercivity

(1) To obtain the rc spectrum of a rock sample, it is necessary to extract the (c.f.)  $R_{rem}$  decay curve from the back-field curve which, in fact, represents the composite spectrum of two superimposed curves: the decay curve of the initial polarity remanence ( $R_{if}$ ) and the re-acquisition curve of the opposite polarity remanence ( $R_{of}$ ).

(2) The rc spectrum can be analyzed in great detail by obtaining a family of  $R_{rem}$  decay curves derived from incremental  $R_{if}$  values.

(3) Comparison of  $R_{if}$  and  $R_{rem}/R_{if}$  curves reveals valuable information about interactive fields within samples:

a) interaction among magnetic carriers occurs in all samples studied including red siltstones where the main magnetic carrier is hematite.

b) the effect of the interaction can be defined by a new parameter 'the crossing point' with its two co-ordinates:  $F_{cp}$  and  $R_{cp}$ .

c)  $F_{cp}$  can be used to estimate the magnitude of the interacting fields.

d)  $R_{cp}$  can be used as a qualitative measure of the effect of interaction.

(4) The  $R_{cp}$  curves show that the effect of the interactive fields is the greatest at the low end of the rc spectrum.

(5) From this preliminary study, it would appear that the  $R_{cp}$  varies among, but remains virtually constant within, rock types; thus the possibility of classifying rock types according to their  $R_{cp}$ .

(6) The saturation remanence/natural remanence ratio is greater than 400 in all samples studied and commonly greater than 1000 indicating that natural rocks are normally magnetized to a very small fraction only of their potential ability to acquire and retain remanences of much larger intensities than those produced by the earth's field.

(7) Since NRMs are commonly composed of two or more individual remanences, the ratio of  $R_{if}$ /individual remanence is likely to be even greater than the  $R_{if}$ /NRM ratio; an exception to this rule might occur if two individual remanences were of opposite polarities.

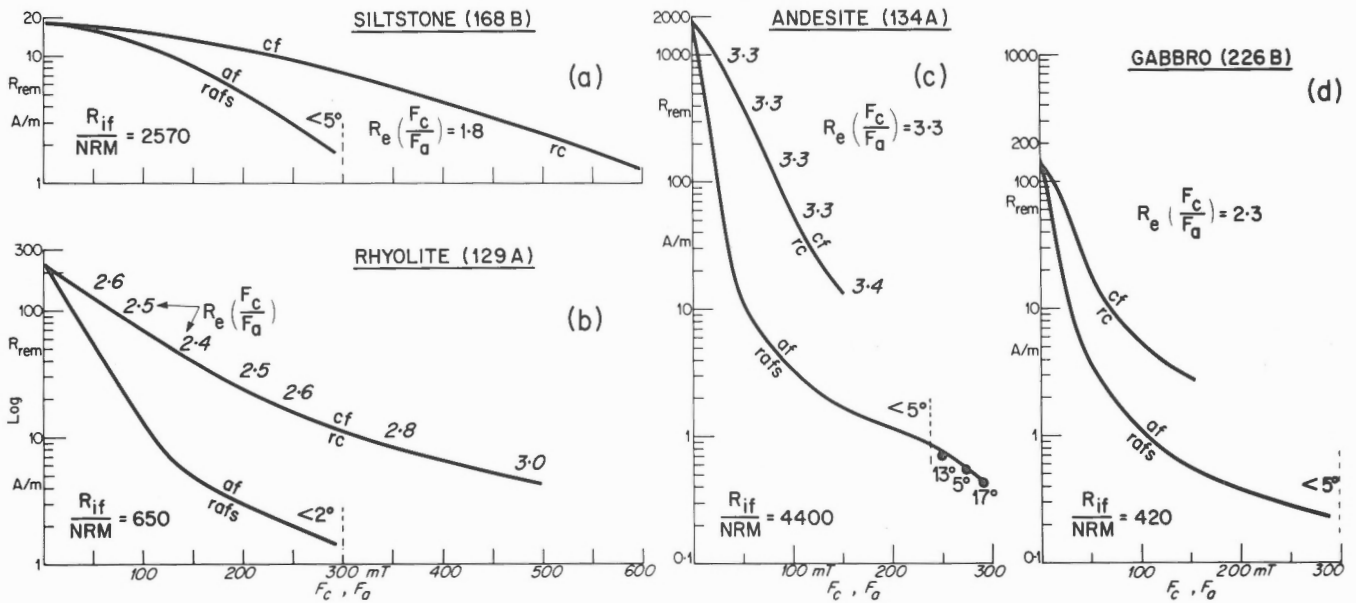


**Figure 11.** Results obtained from different types of rocks: (a) is from site 26 of Roy and Anderson (1981); (b), (c) and (d) are from sites 12, 13 and 10 respectively from Roy et al. (1979). The  $R_e$  and  $R_{if}/NRM$  are shown. The deviations from the initial direction which occurred in (c) at 250 mT and higher are shown. In all other instances, the direction remained within the limits shown (up to the  $F_a$  defined by the dashed vertical marker). All curves shown have been derived from a remanence produced in a  $F_c$  of 1200 mT.

(8) The findings described in (4), (6), (7), (9) and (22) have a considerable impact on the procedure to be used in treatments by alternating fields.

### Remanence a.f. stability

(9) The a.f. treatments are more efficient than c.f. treatments in unlocking the remanence, substantiating the need to differentiate between rafs and rc.

(10) The above is evident in a graphical analysis: the rafs spectrum always lies to the left of (or below) the rc spectrum when a common field scale is used for both  $F_a$  and  $F_c$ .

(11) A relationship between rafs and rc is established by calculating the ratio effectiveness ( $R_e$ ); the ratio is readily determined by measuring the respective  $F_a$  and  $F_c$  required to reduce the saturation remanence to a certain  $R_{rem}$  level, that is, where (c.f.)  $R_{rem} = (a.f.) R_{rem}$ . The ratio can be more explicitly described as  $R_e(F_c/F_a)$ .

(12)  $R_e$  varies according to rock types.

(13)  $R_e$  is nearly constant within a rock type.

(14) Throughout the measurably rafs and rc spectra,  $R_e$  is virtually constant in most rock types but may vary by as much as 25% in certain others.

(15) Variation in  $R_e$  may, in some instances, be indicative of a variable range of grain size magnetic carriers and, in other instances, indicative of the presence of two different types of carriers, e.g. magnetite and hematite.

(16) As further data become available, it is conceivable that  $R_e$  could be used as a rock type index.

### Alternating field

(17) A.f. treatments do not demagnetize rock samples. On the contrary, applied  $F_a$  values usually being in the order of 1 to 300 mT, magnetize the individual magnetic carriers to much larger intensities ( $R_{if}$ ) than those (NRM) acquired in the earth's field (<0.06 mT).

(18) This means that when samples are treated in a  $F_a$  of say 50 mT, some of the magnetic carriers will commonly acquire remanences with intensities 1000 (or more) times larger than the (sought) remanence imprinted by the earth's paleofield.

(19) The success and efficacy of the a.f. technique lie in the randomization of these large intensity vectors so that, ideally, their sum is vectorially cancelled, that is, their resultant vector equals zero.

(20) It should be realized that the randomization effected at a given a.f. treatment step is destroyed upon application of a subsequent treatment to a higher  $F_a$ ; thus the randomization process must be renewed repeatedly.

(21) With each successively higher  $F_a$  step, the ratio of unlocked – low rafs – high intensities/locked – high rafs – low intensity (or potential/sought) remanences increases.

(22) Consequently, to isolate a high coercivity remanence, a high degree of randomization of the low coercivity vectors is required, as seen from a compounding effect of especially (6), (7), (17) and (18).

(23) The required efficacy of the randomizing process can be estimated by considering the following:

a)  $R_{if}/NRM$  ratios of 1000 to 10 000 are common.

b) certain remanences may contribute as little as 1% of

the NRM (e.g. the hematite remanence in a sample carrying both hematite and larger intensity magnetite carriers).

c) as a rule of thumb, to define the three orthogonal components of a remanence with reasonable accuracy, the signal to noise ratio — (in this instance, sought remanence vector/resultant vector of  $R_{if}$ ) — should be in the order of 10 to 20.

A combination of a, b, and c indicates that the randomization factor (resultant/sum of a.f. produced vectors) may need to be, in many instances, in the order of  $10^{-6}$  to  $5 \times 10^{-8}$ .

(24) Desirable features of an a.f. randomizer are: a) exponential (-like) decay ramp, b) high frequency, c) a tumbler attachment.

The first two tend to improve the randomization factor while c) by improving the efficacy of the randomizer effectively increases  $R_e$  and thus extends the coercivity range that can be investigated.

### ***NRM detection***

(25) One of the requirements for correctly interpreting a.f. results is to ensure that the NRM coercivity spectrum has been investigated in its entirety.

(26) The extent of the rc spectrum can be determined directly from the (c.f.)  $R_{rem}$  curves. The advantage of using c.f. experiments is that, technically, larger  $F_c$  than  $F_a$  can be attained. This is very useful where a substantial portion of the remanence resides in medium to high coercivity carriers (e.g. redbeds). However, because (c.f.)  $R_{rem}$  curves are derived from vector subtraction, the spectrum cannot be accurately defined much below 1% of saturation remanence.

(27) Because of the randomization feature, (a.f.)  $R_{rem}$  curves can be accurately defined to a very small percentage of saturation remanence, usually 0.1% and often even lower especially if most of the remanence is located in low to medium rafs carriers (e.g. igneous rocks). With the relationship  $R_e$ , the rafs spectrum can then be used to estimate the extent of the rc spectrum.

(28) Monitoring of vector (direction) changes during a.f. treatment of the saturation remanence is also a most effective means of establishing the extent of the rafs spectrum and thus of ascertaining that all NRM components have been investigated.

### ***Terminology***

(29) With respect to a.f. treatments, demagnetization (demagnetizer) should be replaced by randomization (randomizer).

(30) Distinction should be made between remanence coercivity (rc) and remanence a.f. stability (rafs).

(31) Thus, the term rcf (remanence coercive field) frequently used (even by this author) should be replaced by rafs.

(32) The term MDF (median destructive field) should be

replaced by MRF (median randomizing field) with subscripts S and N to distinguish between saturation remanence and NRM.

(33)  $R_e$  should be used to describe the ratio effectiveness (particular to an a.f. randomizer), that is, the ratio of the fields — continuous ( $F_c$ )/alternating ( $F_a$ ) — required to reduce a remanence to a certain level.

(34)  $R_{cp}$  and  $F_{cp}$  are the co-ordinates of 'the crossing point' parameter which is a qualitative measure of the interacting fields.

(35)  $R_{if}$  is the (not necessarily saturation) remanence produced in laboratory by the initial application of a continuous field ( $F_c$ ).

(36)  $R_{rem}$  is the remanence remaining (of a  $R_{if}$ ) after application of a continuous field of opposite polarity ( $-F_c$ ) or an alternating field ( $F_a$ ); the respective treatments being identified as (c.f.)  $R_{rem}$  and (a.f.)  $R_{rem}$ .

In summary, considering the drastic measures imposed upon the magnetic carriers when a specimen is subjected to a.f. treatments, it is amazing that the technique is at all successful for the analysis of the NRM. Had the early workers realized all the odds against its fruitful application, the technique might not have been developed. As demonstrated, the remanence intensities produced during the treatment are commonly  $10^3$  to  $10^4$  larger than the NRM intensities. This means that in order to investigate the remanence coercivity spectrum of the NRM in its entirety, those intensity vectors generated during treatment may need to be randomized to better than 1 part in a million. Care in both design and operating procedure of an a.f. randomizer is required to attain such a goal.

The relationship ( $R_e$ ) between the remanence coercivity and remanence a.f. stability spectra permits one to make use of either (or alternate between) c.f. and a.f. experiments. This combination provides one with a means of analyzing in more detail practically any part of the remanence coercivity spectrum of the sample. Both methods are non-destructive and the experiments can be repeated at will.

It should not be construed from this study that all components of remanence naturally imprinted into a sample can be recognized and sorted out by a.f. treatments alone. However, a.f. results can compliment results obtained by other means, such as thermal and chemical, and, in certain instances as shown here, may reveal information that could not be uncovered by those other means.

### **ACKNOWLEDGMENT**

I am greatly indebted to David Dunlop of the Geophysics Laboratory, University of Toronto, for a thorough review of the initial manuscript.

## REFERENCES

### Bailey, M.E. and Dunlop, D.J.

1983: Alternating field characteristics of pseudo-single-domain (2-14 m) and multidomain magnetite; *Earth and Planetary Science Letters*, v. 63, p. 335-352.

### Black, R.F.

1964: Paleomagnetic support of the theory of rotation of the western part of the island of Newfoundland; *Nature*, v. 202, p. 945-948.

### Buchan, K.L. and Dunlop, D.J.

1976: Paleomagnetism of the Haliburton intrusions: superimposed magnetizations, metamorphism, and tectonics in the late Precambrian; *Journal of Geophysical Research*, v. 81, p. 2951-1967.

### Buchan, K.L., Berger, G.W., McWilliams, M.O., York, D. and Dunlop, D.J.

1977: Thermal overprinting of natural remanent magnetization and K/Ar ages in metamorphic rocks; *advances in Earth and Planetary Sciences*, v. 1, p. 169-178.

### Cisowski, S.

1981: Interacting vs non-interacting single domain behavior in natural and synthetic samples; *Physics of the Earth and Planetary Interiors*, v. 26, p. 56-62.

### Dankers, P.H.M.

1978: Magnetite properties of dispersed natural iron-oxides of known grain-size; Ph.D. Thesis, State University of Utrecht, 142 p.

### Dankers, P.

1981: Relationship between median destructive field and remanent coercive forces for dispersed natural magnetite, titanomagnetite and hematite; *Geophysical Journal of the Royal Astronomical Society*, v. 64, p. 447-461.

### Dunlop, D.J.

1971: Magnetic properties of fine-particle hematite; *Annales de Géophysique*, v. 27, p. 269-293.

### Dunlop, D.J.

1986: Coercive forces and coercivity spectra of submicron magnetites; *Earth and Planetary Science Letters*, v. 78, p. 288-295.

### Dunlop, D.J. and West, G.F.

1969: An experimental evaluation of single domain theories; *Reviews of Geophysics*, v. 7, p. 709-757.

### Hartstra, R.L.

1982a: A comparative study of the ARM and  $I_{st}$  of some natural magnetite of MD and PSD grain-size; *Geophysical Journal of the Royal Astronomical Society*, v. 71, p. 497-518.

### Hartstra, R.L.

1982b: Grain-size dependence of initial susceptibility and saturation magnetization-related parameters of four natural magnetites in the PSD-MD range; *Geophysical Journal of the Royal Astronomical Society*, v. 71, p. 477-495.

### Kent, D.V. and Opdyke N.D.

1978: Paleomagnetism of the Devonian Catskill red beds: evidence for motion of the coastal New England-Canadian Maritime region relative to cratonic North America; *Journal of Geophysical Research*, v. 83, p. 4441-4450.

### Lapointe, P.L., Roy, J.L. and Morris, W.A.

1978: What happened to the high-latitude paleomagnetic poles? *Nature*, v. 273, p. 655-657.

### Levi, S. and Merrill, R.T.

1978: Properties of single domain, pseudo-single-domain and multidomain magnetite; *Journal of Geophysical Research*, v. 83, p. 309-323.

### Park, J.K.

1984: Alternating field treatment of paleomagnetic samples: some results on the effectiveness of "tumbling" over "non-tumbling"; *Earth Physics Branch Open File 84-1*, Ottawa, Canada.

### Roy, J.L. and Anderson, P.

1981: An investigation of the remanence characteristics of three sedimentary units of the silurian Mascarene Group of New Brunswick, Canada; *Journal of Geophysical Research*, v. 86, p. 6351-6368.

### Roy, J.L. and Lapointe, P.L.

1978: Multiphase magnetizations; *Physics of the Earth and Planetary Interiors*, v. 16, p. 20-37.

### Roy, J.L. and Robertson, W.A.

1978: Paleomagnetism of the Jacobsville Formation and the apparent polar path for the interval -1100 to -670 m.y. for North America; *Journal of Geophysical Research*, v. 83, p. 1289-1304.

### Roy, J.L., Anderson, P. and Lapointe, P.L.

1979: Paleomagnetic results from three rock units of New Brunswick and their bearing on the Lower Paleozoic tectonics of North America; *Canadian Journal of Earth Sciences*, v. 16, p. 1210-1227.

### Roy, J.L., Reynolds, J. and Sanders, E.

1973: An alternating field demagnetizer for rock magnetism studies; *Publications of the Earth Physics Branch*, v. 44, no. 3, p. 37-45.

### Seguin, M.K., Rao, K.V. and Arnal, P.

1981: Paleomagnetic study of Cambrian Potsdam Group sandstones, St. Lawrence Lowlands, Quebec; *Earth and Planetary Science Letters*, v. 55, p. 433-449.



